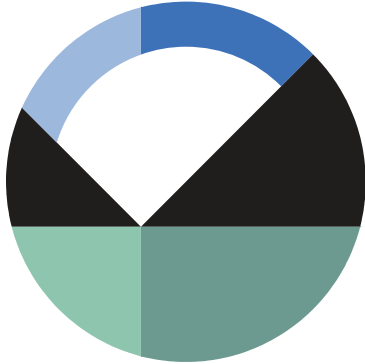


Add-In: Gas Consumption and Exothermic Reactions



GEOSLOPE International Ltd. | www.geoslope.com

1200, 700 - 6th Ave SW, Calgary, AB, Canada T2P 0T8
Main: +1 403 269 2002 | Fax: +1 888 463 2239

Introduction

The production of acid mine drainage from the oxidation of sulfidic materials, particularly pyrite, is an environmental concern. Pyrite oxidation is an exothermic reaction in which heat is generated as the sulfidic materials are changed from insoluble sulfides into highly soluble sulfates. Many studies have been conducted to simulate this reaction to better understand the physical processes involved in the generation of acid mine drainage and to establish preventative and mitigation methods, such as soil cover systems. Many of the models require multi-physics capabilities, as the exothermic reaction typically requires coupled gas, heat, water, air, and solute transfer processes (e.g., Jaynes et al., 1984, Lefebvre et al., 2001, and Pantelis et al., 2002). The purpose of this example is to illustrate how to use the Gas Consumption and Exothermic Reactions add-in to simulate the exothermic oxidation process. The add-in does not currently consider the solute process, in which the pyritic materials are converted to a soluble form. Instead, only the coupled gas, heat, water, and air transfer processes are simulated.

Background

The oxidation of sulfidic materials is an exothermic reaction that leads to the development of acid mine drainage. The simulation of this process requires multi-physics capabilities to consider the various complex reactions taking place. The rate at which this oxidation process takes place is dependent on the available oxygen gas concentration, temperature, pH, and sulfide concentration within the waste rock (Jaynes et al., 1984).

The oxidation process can be modeled as an irreversible first-order reaction for which the reaction rate law reads:

$$\frac{dC}{dt} = -K_r^* C$$

Equation 1

where C is the mass concentration of the gas, t is the time, and K_r^* is the bulk reaction rate coefficient. Reformulating and integrating this equation leads to the integrated first-order rate law, which can be used to compute the change in mass over a given time step. The energy generated from the oxidation process over the time step (ΔE) is equal to the negative product of the heat of oxidation (H_c) and the change in mass (ΔM), such that:

$$\Delta E = -H_c \Delta M = -H_c \theta_{eq} dC / \Delta t$$

Equation 2

where θ_{eq} and the heat of oxidation (H_c) ranges from 360 – 400 kJ/mole of oxygen, or 11250 – 12500 kJ/kg of oxygen. The generated energy can be converted into a boundary heat flux by dividing the energy by the time step, and multiplying by the element thickness:

$$q_t = \Delta E \Delta z / \Delta t$$

Equation 3

where Δz is the element thickness, which is herein assumed equal to one. The use of the heat flux boundary condition ensures that the volume is computed correctly in the heat generation calculation. It must be noted that the rate at which oxidation takes place is dependent on various factors, including the available oxygen gas concentration in the pore-space and the temperature, which can be taken into account through limiting functions (Jaynes et al., 1984).

Numerical Experiment

The capabilities of the Gas Consumption and Exothermic Reactions add-in are evaluated with a 50 m-high waste rock dump. As shown in Figure 1, the waste rock dump is assumed mostly non-reactive, with a 5 m layer of oxidizing material across the mid-section. For the sake of simplicity, the air temperature is set constant at 20°C. The initial oxygen gas concentration of both materials is set equal to 280 g/m³, and a constant gas concentration boundary condition of 280 g/m³ is applied at the surface.

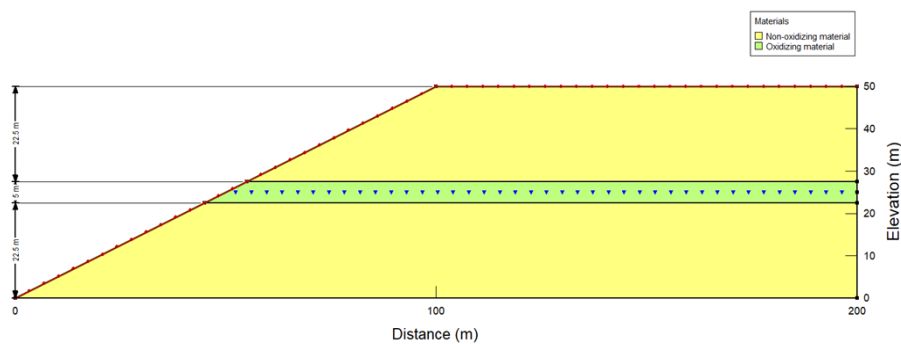


Figure 1. Model configuration.

The project file contains three analyses that illustrate the use of the add-in in one- and two-dimensional scenarios (Figure 2). The first one-dimensional scenario focuses on the oxidizing material alone, whereas the second scenario focuses on the oxidizing material and the non-reactive material response. The third analysis considers the oxidizing material and non-reactive material response in a two-dimensional domain. The physics in each analysis are identical. As shown in Figure 3, the Air with free convection, Water, Heat with forced air convection, and Gas (oxygen) with advection-dispersion physical processes are considered.



Figure 2. Analysis tree of the project.

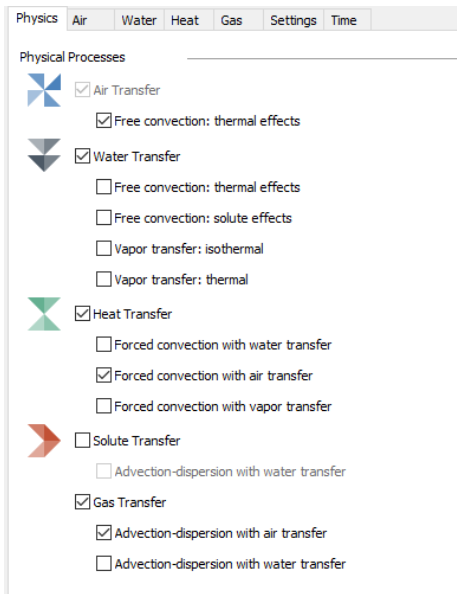


Figure 3. Physics tab for each analysis.

The reactive and non-reactive material properties are kept identical, with the exception of the Bulk Reaction Rate function, which is defined with the Temperature and Concentration Reaction Rate Limits function of the Gas Consumption and Exothermic Reactions add-in. The inputs of the function are the Optimal Reaction Rate, as well as the Temperature Limiting Function Name and the Gas Concentration Limiting Function Name, which must read as follows:

`Functions.Boundary.Thermal.ModFns.'TempModifierFunction'`

`Functions.Boundary.Gas.ModFns.'GasConcModFunction'`

The Temperature Limiting Function accounts for the effect of temperature on the bacterial activity, which is responsible for oxidation. As shown in Figure 4, the limiting function decreases when the temperature is not within a desirable range. The Gas Concentration Limiting Function, on the other hand, accounts for the effect of oxygen concentration on the bacterial activity (Figure 5). In this example, the Optimal Reaction Rate is set equal to 1×10^{-7} /s.

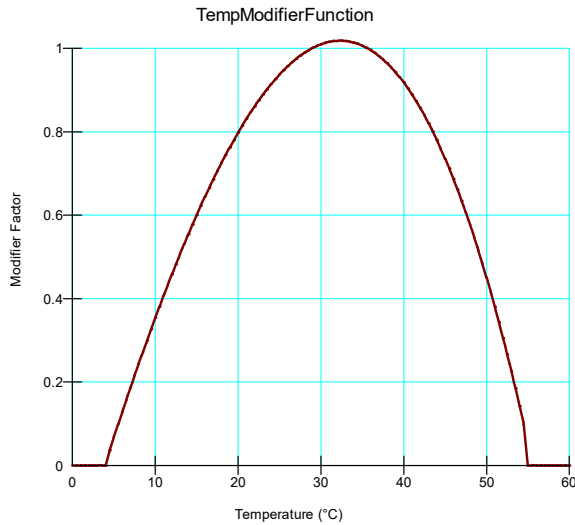


Figure 4. Thermal modifier function to impose limits on the reaction rate based on soil temperature.

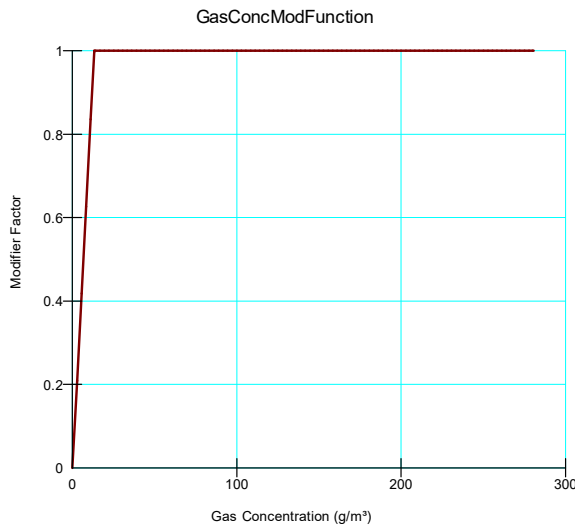


Figure 5. Gas concentration modifier function to impose limits on the reaction rate based on available oxygen concentration in the pore-space.

The energy generated by the oxidation process is accounted for by the First Order Exothermic Heat Flux function of the Gas Consumption and Exothermic Reactions add-in. The only input is the Heat of Oxidation, which is herein set equal to -1.258×10^7 kJ/Mg of oxygen. To define this function as a boundary condition, a heat flux boundary condition is applied, and the function option is selected.

The type of function is then set to Add-In Function, the Add-In is set to Gas Consumption and Exothermic Reactions, and the Function is set to First Order Exothermic Heat Flux (Figure 6). The boundary condition must then be applied to the desired region. This ensures that the heat flux is applied to the element area, so that the heat rate is calculated and applied to the volume.

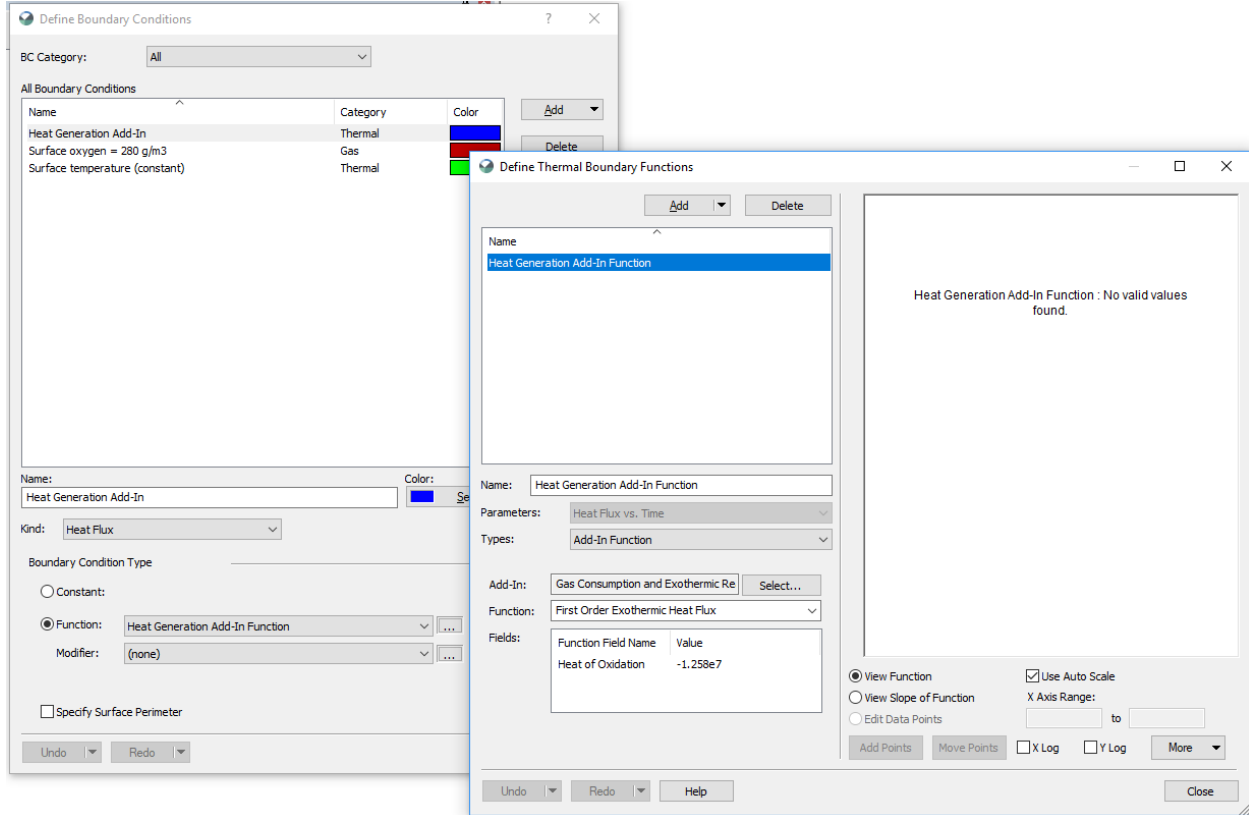


Figure 6. Definition of the First Order Exothermic Heat Flux function boundary condition.

Results and Discussion

Figure 7 and Figure 8 show plots of gas concentration and temperature versus time for each of the scenarios at the center of the oxidizing material on the right-hand side of the domain. The simulated results of the first scenario are shown to be in close agreement with hand calculations using Equation 1 and Equation 3. As expected, the oxidation process follows the first-order reaction law, and the gas concentration decreases exponentially. The heat generated by the reaction produces an exponential increase in temperature, which tends towards a maximum of 21°C. Given the gas concentration limits placed on the reaction rate coefficient, the heat generated by the oxidation process decreases to zero as the oxygen concentration falls below 13 g/m³.

In scenarios 2 and 3, on the other hand, the domains include the non-reactive material, and the simulated oxygen concentrations differ significantly. This can be ascribed to the oxygen influx from the surrounding non-reactive material. In essence, the oxygen moves through the soil pores, towards the oxidizing material, via both advection and diffusion processes. This allows for more heat

generation, which gives rise to higher temperatures. If the advection-dispersion option is turned-off and the diffusion coefficient is decreased to a negligible value, most of the oxygen is removed by oxidation and the simulated oxygen concentration tends towards that observed in the first scenario.

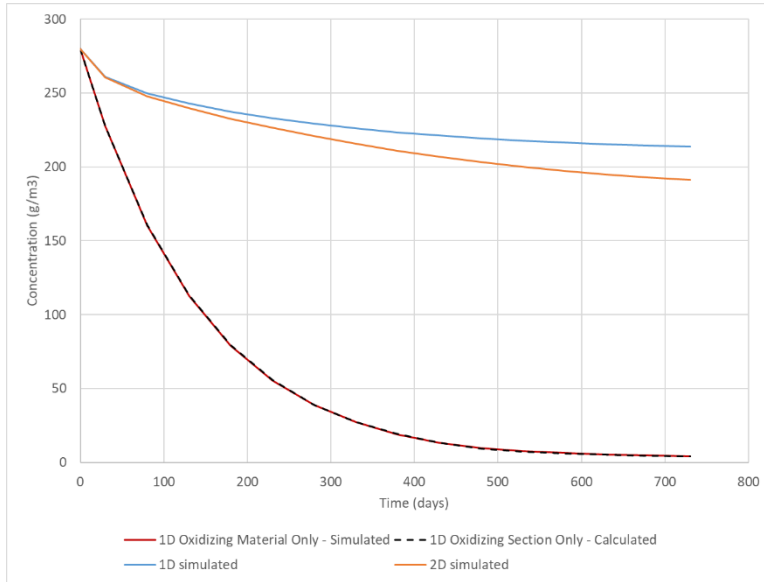


Figure 7. Gas concentration versus time for each simulated scenario.

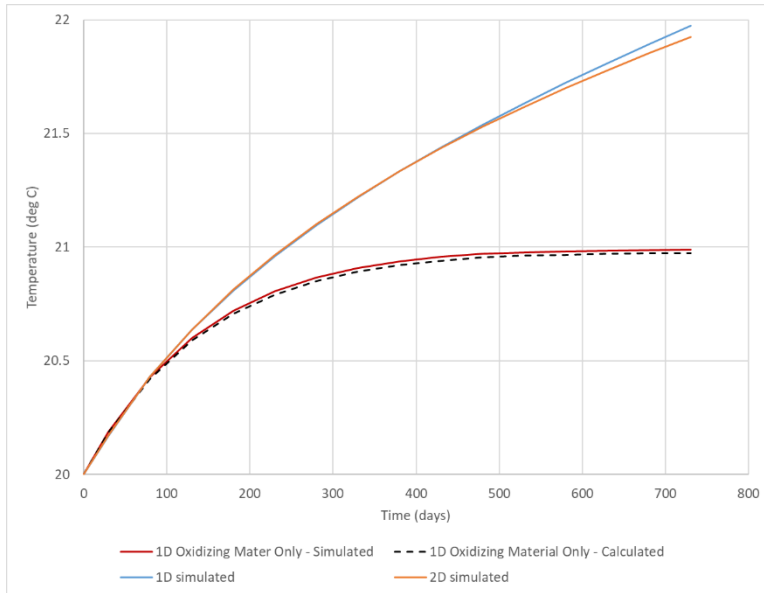


Figure 8. Temperature versus time for each simulated scenario.

Figure 9 shows the gas concentration contours for the two-dimensional analysis at the end of the two year period. As expected, the gas concentration is lowest in the region furthest from the boundary, at the bottom edge of the right-hand side of the domain. Figure 10 shows the temperature contours at the same point in time, and reveals that the temperature within the reactive material is

approximately constant at 22°C. There is, however, a small region close to the sloped surface where temperatures are slightly higher due to constant oxygen replenishment.

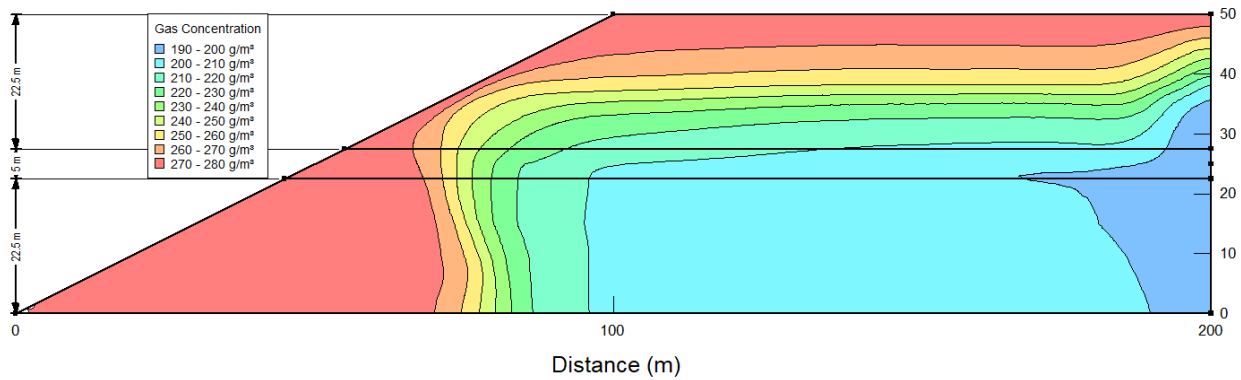


Figure 9. Gas concentration contours at the end of the 2 year period in the 2D scenario.

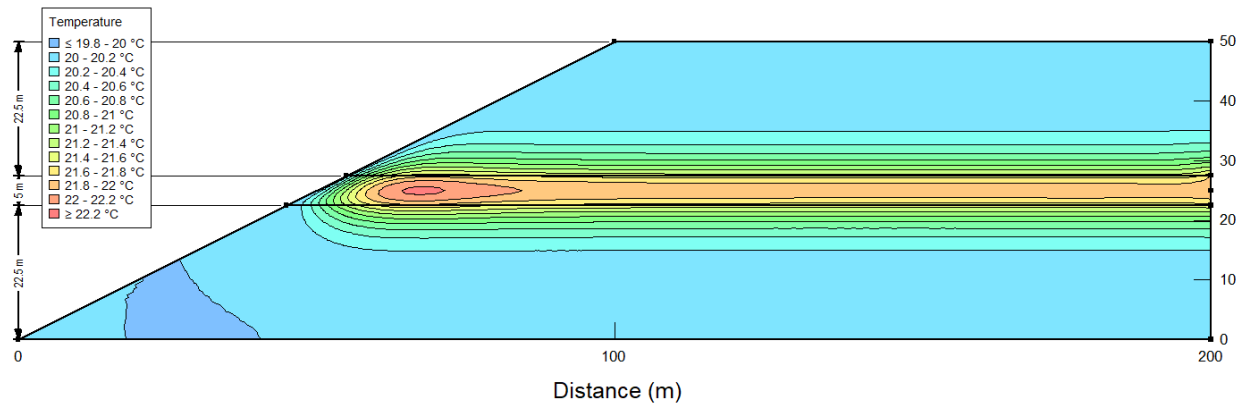


Figure 10. Temperature contours at the end of the 2 year period in the 2D scenario.

Summary and Conclusion

This illustrative example shows how the Gas Consumption and Exothermic Reactions add-in can be used to simulate exothermic reactions. This example, in particular, considers the oxidation of sulfidic materials within a waste rock dump. The influence of various cover systems on reducing the heat generation and oxidation experienced within the waste rock can be considered in further analyses.

References

- Jaynes, D.B., Rogowski, A.S., and Pionke, H.B. 1984. Acid mine drainage from reclaimed coal strip mines: 1. model description. *Water Resources Research* 20 (2): 233-242.
- Lefebvre, R., Hockley, D., Smolensky, J., and Lamontagne, A. 2001. Multiphase transfer processes in waste rock piles producing acid mine drainage – 2. applications of numerical simulation. *Journal of Contaminant Hydrology* 52: 165-186.

Pantelis, G., Ritchie, A.I.M., and Stepanyants, Y.A. 2002. A conceptual model for the description of oxidation and transport processes in sulphidic waste rock dumps. *Applied Mathematical Modelling* 26: 751-770.